Diabetologia (2007) 50:1997–2007
DOI 10.1007/s00125-007-0728-7

ARTICLE

Ablation of the gene encoding p66^{Shc} protects mice against AGE-induced glomerulopathy by preventing oxidant-dependent tissue injury and further AGE accumulation

S. Menini · C. Iacobini · C. Ricci · G. Oddi · C. Pesce · F. Pugliese · K. Block · H. E. Abboud · M. Giorgio · E. Migliaccio · P. G. Pelicci · G. Pugliese

Received: 1 March 2007 / Accepted: 23 April 2007 / Published online: 5 July 2007

Abstract
Aims/hypothesis AGEs have been implicated in renal disease associated with ageing, diabetes and other age-related disorders. Reactive oxygen species (ROS) promote formation of AGEs, which cause AGE-receptor-mediated ROS generation with activation of signalling pathways leading to tissue injury and further AGE accumulation. ROS generation is regulated by the Src homology 2 domain-containing transforming protein C1 (Shc1) isoform p66^{Shc}, whose deletion has been shown to protect from tissue injury induced by ageing, diabetes, hyperlipidaemia and ischaemia-reperfusion by preventing oxidative stress. This study was aimed at assessing the role of p66^{Shc} in the modulation of oxidative stress and oxidant-dependent renal injury induced by AGEs.
Methods For 10 weeks, male *p66^{shc}* knockout (KO) and wild-type (WT) mice were injected with 60 μg/day albumin modified or unmodified by N^{ε}−(carboxymethyl) lysine (CML). Mice were then killed for the assessment of renal function and structure, as well as systemic and renal tissue oxidative stress.
Results Upon CML injection, KO mice, in contrast to WT mice, showed no or only mild forms of proteinuria, glomerular hypertrophy, mesangial expansion, glomerular sclerosis, renal/glomerular cell apoptosis and extracellular matrix upregulation. Moreover, KO mice had lower circulating and tissue AGEs than WT mice and unchanged plasma isoprostane 8-epi-prostaglandin-$F_{2\alpha}$ levels, renal/glomerular CML, 4-hydroxy-2-nonenal, AGE receptor and NAD(P)H oxidase 4 (NOX4) content (and expression of the corresponding genes), and nuclear factor κB activation (NFκB). Mesangial cells from KO mice exposed to CML showed no or slight increase in ROS levels and NFκB activation, again at variance with WT cells.
Conclusions/interpretation These data indicate that p66^{Shc} participates in the pathogenesis of AGE-dependent glomerulopathy by mediating AGE-induced tissue injury and further AGE formation through ROS-dependent mechanisms involving NFκB activation and upregulation of *Nox4* expression and NOX4 production.

Keywords AGEs · AGE receptors · Apoptosis · Extracellular matrix · Nephropathy · Oxidative stress · p66^{Shc} · NAD(P)H oxidase · NOX4 · Nuclear factor κB

Electronic supplementary material The online version of this article (doi:10.1007/s00125-007-0728-7) contains supplementary material, which is available to authorised users.

S. Menini · C. Iacobini · C. Ricci · G. Oddi · F. Pugliese · G. Pugliese (✉)
Department of Clinical Sciences, 'La Sapienza' University, Viale del Policlinico, 155-00161 Rome, Italy
e-mail: giuseppe.pugliese@uniroma1.it

C. Pesce
DISTBIMO, University of Genoa Medical School, Genoa, Italy

K. Block · H. E. Abboud
Department of Medicine, Division of Nephrology, University of Texas Health Science Center, San Antonio, TX, USA

M. Giorgio · E. Migliaccio · P. G. Pelicci
Department of Experimental Oncology, European Institute of Oncology, Milan, Italy

Abbreviations

CM-H_2DCFDA	5-(and-6)-chloromethyl-2′,7′-dichlorodihydrofluorescein diacetate
CML	N^{ε}−(carboxymethyl) lysine
COL4A1	collagen IV α1 chain
ECM	extracellular matrix
fMA	fractional mesangial area
FN1	fibronectin
GAL3	galectin-3
GAPDH	glyceraldehyde phosphate dehydrogenase
Grb2	growth factor receptor bound protein
HNE	4-hydroxy-2-nonenal
KO	knockout
MAPK	mitogen-activated protein kinase
mGA	mean glomerular area
mGV	mean glomerular volume
mMA	mean mesangial area
MSA	mouse serum albumin
NFκB	nuclear factor κB
NOX4	NAD(P)H oxidase 4
OD	optical density
PAS	periodic acid–Schiff
PGF	prostaglandin F
Rac1	Ras-related C3 botulinum toxin substrate 1
ROS	reactive oxygen species
Shc1	Src homology 2 domain-containing transforming protein C1
Sos1	son of sevenless 1 protein
WT	wild-type

Introduction

Nonenzymatic glycation with AGE formation has been implicated in the pathogenesis of diabetic nephropathy and other long-term complications of diabetes, based on the demonstration that AGE injection in experimental animals was capable of producing renal and vascular alterations similar to those occurring in diabetes [1–3] and that the use of inhibitors of AGE formation and/or crosslinking prevented experimental diabetic glomerulopathy and cardiovascular disease [4–7]. AGEs were shown to accumulate also in ageing [8, 9] and age-related conditions such as central obesity, dyslipidaemia and hypertension [10–12], clustering with impaired glucose metabolism in the setting of metabolic syndrome and associated with systemic inflammation and increased risk of renal and cardiovascular disease [13, 14].

Increased amounts of AGEs are formed under these conditions due to several mechanisms, including enhanced carbohydrate and/or lipid substrate availability, increased oxidative and nonoxidative metabolism, impaired detoxification caused by consumption of cofactors of detoxifying enzymes and, in the case of associated renal failure, reduced kidney clearance [15]. Enhanced mitochondrial superoxide production, resulting from excess glucose disposal and causing diversion of glucose flux towards the AGE-precursor methylglyoxal via inhibition of glyceraldehyde phosphate dehydrogenase (GAPDH), is now considered to be the main mechanism of AGE formation in diabetes [16]; in ageing individuals, moreover, a less efficient electron transport in the mitochondrial respiratory chain has been observed [17]. In addition, protein kinase C activation, which results from superoxide-dependent GAPDH inhibition via increased diacylglycerol formation, is responsible for the phosphorylation of Ras-related C3 botulinum toxin substrate 1 (Rac1) GTPase, an activator of the reactive oxygen species (ROS)-generating enzyme NAD(P)H oxidase [18]. Thus, in addition to nonoxidatively formed methylglyoxal-derived AGEs, carbonyl precursors and AGEs derived from oxidative reactions, such as glyoxal, pentosidine and N^{ε}−(carboxymethyl) lysine (CML), are also detected in sera and tissues of these patients [15, 19].

Apart from displaying direct, physico-chemical effects, such as trapping and crosslinking of macromolecules, AGEs exert indirect, biological effects, mediated by cell surface receptors. Receptors for AGEs (RAGEs) have a dual function, since they are involved in AGE removal, and also in AGE-induced cell activation [20], triggered by RAGE-mediated ROS generation via mitochondrial and cytosolic pathways involving the electron transport chain and NAD(P)H oxidase, respectively [21]. ROS cause further AGE formation as well as $p21^{ras}$/mitogen-activated protein kinase (MAPK)-dependent activation of transcription factors such as nuclear factor κB (NFκB) [22, 23] and the modulation of expression of genes encoding several cytokines, thus leading to the dysregulated tissue remodelling underlying all the above pathological conditions [24, 25]. The prevention of AGE-induced vascular dysfunction by antioxidant treatment both in vitro [26, 27] and vivo [28, 29] suggest a pivotal role for AGE/RAGE-mediated ROS generation in the pathogenesis of AGE-dependent tissue injury.

The proto-oncogene Src homology 2 domain-containing transforming protein C1 locus (*SHC*, also known as *SHC1*) encodes three SHC isoforms, $p46^{Shc}$, $p52^{Shc}$ and $p66^{Shc}$. Unlike $p52^{Shc}$ and $p46^{Shc}$, $p66^{Shc}$ is not involved in Ras activation and cell proliferation [30]. Conversely, by virtue of its unique amino-terminal collagen homology 2 domain, $p66^{Shc}$ controls oxidative stress response and life span. In fact, $p66^{Shc}$ knockout (KO) mice showed increased life span and resistance to paraquat treatment compared with wild-type (WT) mice [31]. Moreover, $p66^{Shc}$ was shown to regulate steady-state intracellular ROS levels [32] and to generate proapoptotic hydrogen peroxide in response to

specific stress signals by serving as a redox enzyme that oxidises cytochrome *c* within the mitochondria [33]. *p66*^{Shc} KO mice showed reduced circulating and tissue ROS levels and ROS-mediated damage in response to diabetes, ageing, hyperlipidaemia, ischaemia and ischaemia-reperfusion, as compared with the corresponding WT mice [34–38]. Likewise, cells from KO mice exhibited lower ROS levels and reduced cell death rate vs cells from WT animals when exposed to hydrogen peroxide or ultraviolet light [31] or conditions mimicking hyperglycaemia and ischaemia [34, 37]. As a consequence, *p66*^{Shc} KO mice were found to be protected from diabetic glomerulopathy and cardiomyopathy, endothelial dysfunction associated with ageing, early atherogenesis induced by high-fat diet and tissue damage produced by ischaemia and ischaemia-reperfusion [34–38]. Moreover, *p66*^{Shc} ablation was found to reduce AGE formation in diabetic animals [34].

This study was aimed at verifying the hypotheses that: (1) AGE-dependent oxidative stress represents the main mechanism of AGE-induced renal injury; (2) p66^{Shc} plays a central role in modulating AGE-induced ROS generation; and (3) NAD(P)H oxidase is involved in the regulation of ROS levels by p66^{Shc}, in addition to mitochondrial pathways [33].

Materials and methods

Animal studies These studies were approved by the local ethical committee. Adult (aged 2 months) male *p66*^{shc} KO and coeval SV/129 WT mice (Charles River, Milan, Italy) were injected with either CML-modified or unmodified mouse serum albumin (MSA). Both preparations were given intraperitoneally at the daily dose of 60 μg for 10 weeks, based on previously published studies [39]. Untreated mice of both genotypes served as normal controls. The animals were housed and cared for in accordance with the Principles of Laboratory Animal Care (NIH Publication no. 85–23, revised 1985) and national laws, and had free access to water and food. At the end of the 10 week period, the animals were placed in metabolic cages to collect urine. The day after, body weights were recorded, then mice were anaesthetised with ketamine (Imalgene; Merial, Milan, Italy; 60 mg/kg body weight i.m.) and xylazine (Rompum; Bayer, Milan Italy, 7.5 mg/kg body weight i.m.) and a longitudinal incision of the abdominal wall was performed. Animals were then killed by blood withdrawal, a blood sample was collected, and both kidneys were quickly removed, cleaned of the surrounding fat, washed in phosphate-buffered saline and weighed.

Cell culture studies Mesangial cells were isolated from 1-month-old KO and WT mice and characterised as previously described [34]. Cells between the third and the tenth passage were seeded on poly-D-lysine-coated glass coverslips or 100 mm Petri dishes (Falcon; Becton Dickinson, Lincoln Park, NJ, USA) and cultured in DMEM (Sigma, St Louis, MO, USA) supplemented with 17% fetal bovine serum, 2 mmol/l L-glutamine and antibiotics (Flow Laboratories, Irvine, Scotland, UK), at 37°C in a humidified atmosphere consisting of 95% air and 5% CO_2, after which they were incubated for 1 h with MSA or CML at a concentration of 100 μg/ml.

AGE preparation CML was prepared as previously reported [39]. Briefly, 175 mg MSA (Sigma) were incubated in 1 ml of 0.2 mol/l phosphate buffer, pH 7.8, containing 0.15 mol/l glyoxylic acid and 0.45 mol/l sodium cyanoborohydrate, for 24 h at 37°C. CML-modified and unmodified MSA were then dialysed against water for 48 h using 22 μm dialysis membranes, purified several times through endotoxin-removing columns (Detoxi-Gel; Pierce Chemical, Rockford, IL, USA), passed through 22 μm filters and assessed (1) for endotoxin content by the *Limulus* amoebocyte lysate assay (Sigma), (2) for extent of CML modification by the 2,4,6-trinitrobenzene sulfonic acid method and (3) for protein content by the Bradford method using the Bradford dye-binding protein assay kit (Pierce).

Renal function Serum and urine creatinine levels were measured by HPLC, total proteinuria by the Bradford method using the Bradford dye-binding protein assay kit (Pierce) and albuminuria by ELISA using a kit (Mouse Albumin ELISA Quantitation Kit; Bethyl, Montgomery, TX, USA). Values of proteinuria and albuminuria were normalised against urine creatinine concentration [34, 39].

Renal structure A sagittal section of the right kidney was immediately fixed by immersion in phosphate-buffered paraformaldehyde solution [4% (vol./vol.)] and embedded in paraffin. Analysis of renal structure was performed by two pathologists blinded to the group assignment of the specimens on multiple 4 μm sections stained with periodic acid–Schiff (PAS), as previously reported [34, 39]. Sections were evaluated for glomerular sclerosis by a standard semiquantitative analysis and results expressed as glomerular sclerosis index. For morphometric analysis, the areas of at least 60 glomerular tuft profiles per sample were measured, the harmonic mean of the profile area [mean glomerular area (mGA)] was obtained and the mean glomerular volume (mGV) estimated from it. Then, PAS-positive material in each glomerulus was quantified and expressed as the percentage of the glomerular tuft area [fractional mesangial area (fMA)]. Finally, the mean mesangial area (mMA) was calculated by the formula: (fMA × mGA)/100.

Renal/glomerular cell apoptosis Glomerular and tubular cell death rates were assessed in paraffin-embedded sections by immunohistochemistry for active caspase-3 using a rabbit polyclonal IgG antibody (anti-ACTIVE Caspase-3; Promega Italia, Milan, Italy), as previously reported [34, 39]. Positive cells were counted and expressed as percent of total cells. The glomerular cell type undergoing apoptosis was then identified topographically by counterstaining sections with PAS to mark basement membranes [34].

Renal Fn1, Col4a1, Rage, Gal3, Nox4 and $p66^{Shc}$ *mRNA expression* Total RNA was extracted from renal cortex of left kidney by the guanidine thiocyanate–phenol–chloroform method using Trizol reagent (Invitrogen Italia, San Giuliano Milanese, Italy). Transcripts of the genes encoding extracellular matrix (ECM) proteins fibronectin (*Fn1*) and collagen IV α1 chain (*Col4a1*), the AGE receptors RAGE (*Rage*, also known as *Ager*) and galectin-3 (*Gal3*), the renal NAD(P)H oxidase 4 isoform (*Nox4*) and $p66^{Shc}$ were quantified by competitive RT-PCR, as previously reported [34, 39]. Briefly, 1 μg of total RNA was reverse transcribed using a Retroscript kit (Ambion, Austin, TX, USA) and the resulting cDNA was amplified using the following primers: *Fn1* sense: 5′ AGCGGTGTGGTCTACTCTGT 3′, antisense: 5′ GATGCACTGATCTCGGAGCT 3′; *Col4a1* sense: 5′ TAGGTGTCAGCAATTAGGCAGG 3′, antisense: 5′ TCAC TTCAAGCATAGTGGTCCG 3′; *Rage* sense: 5′ CCT GGGAAGCCAGAAATT 3′, antisense: 5′ GCACAGGT CAAGGTCACA 3′; *Gal3* sense: 5′ CACCTGCACCTGGA GTCTAC 3′, antisense:5′ GCACTGGTGAGGTCTATGTC 3′; *Nox4* sense: 5′ GAAGCCCATTTGAGGAGTCA 3′, antisense: 5′ GGGTCCACAGCAGAAAACTC 3′; $p66^{Shc}$ sense: 5′ ACTACCCTGTGTTCCTTCTTTC 3′, antisense: 5′ TCGGTGGATTCCTGAGATACTGT 3′; and β-actin (for normalisation) sense: 5′ TCTAGGCACCAAGGTGTG 3′, antisense: 5′ TCATGAGGTAGTCCGTCAGG 3′. Competitive PCR was performed by using increasing amounts of mutants made by creating a deletion in the original PCR product. After electrophoresis of PCR products, the unknown cDNA : mutant ratio was quantified by scanning densitometry using ImageJ software (available from: http://rsb.info.nih.gov/ij/, last accessed in May 2007) and results were expressed as the ratio of each target to β-actin mRNA level.

Renal/glomerular FN1, COL4A1, RAGE, NOX4 and GAL-3 protein levels Renal content and distribution of ECM proteins, AGE receptors and NOX4 were assessed by immunohistochemistry, as previously reported [34], using rabbit polyclonal antibodies to human FN1 (Sigma), mouse COL4A1 (Abcam, Cambridge, UK), human RAGE (amino acids 42–59; Abcam), recombinant glutathione *S*-transferase–mouse NOX4 (299–515) [40] and a rat monoclonal antibody against human GAL3 [41]. Sections were analysed using the Optimas 6.5 image analysis system (Optimas; MediaCybernetics, Silver Spring, MD, USA) and results are expressed as percentage of glomerular area positive to each protein.

Serum and kidney AGE levels The level of AGEs in serum, urine and kidney cortex extracts was assessed by a competitive ELISA technique, using a mouse monoclonal antibody raised against AGE-modified bovine serum albumin, which also recognises CML [34, 39]. Renal content of the glycoxidation product CML and the lipoxidation product 4-hydroxy-2-nonenal (HNE) was assessed in paraffin-embedded sections by immunohistochemistry, using a biotinylated mouse monoclonal antibody against CML (Wako, Neuss, Germany) and a rabbit antiserum against HNE (Alpha Diagnostic International, San Antonio, TX, USA), respectively [34, 39].

Plasma isoprostane 8-epi-prostaglandin $F_{2\alpha}$ levels Plasma levels of isoprostane 8-epi-prostaglandin $F_{2\alpha}$($PGF_{2\alpha}$), an index of systemic oxidative stress, were determined by ELISA using a commercial kit (Cayman, Ann Arbor, MI, USA) [34].

Renal/mesangial NFκB activation Nuclear protein extracts were obtained from kidney tissue and mesangial cells using a kit (TransFactor Extraction Kit; BD Biosciences Clontech, Palo Alto, CA, USA). The activation of NFκB/p65 was assessed by ELISA using the Mercury TransFactor NFκB p65 kit (BD Biosciences Clontech) [34, 39]. Nuclear translocation of NFκB/p65 in cultured mesangial cells was assessed by immunofluorescence. Briefly, cells were fixed in paraformaldehyde [4% (vol./vol.)] for 5 min at 4°C, permeabilised with Triton X-100 [0.1% (vol./vol.)] for 15 min, treated for 15 min with Image-iT FX signal enhancer (Molecular Probes, Eugene, OR, USA) to block background and incubated overnight at 4°C with a rabbit polyclonal affinity purified antibody against a peptide mapping within the N-terminus of NFκB p65 of human origin (Santa Cruz Biotechnology). After this cells were incubated with a fluorophore-conjugated goat anti-rabbit secondary antibody (Alexa Fluor 488; Molecular Probes) for 1 h at room temperature. Finally, coverslips were mounted using Vectashield mounting medium (Vector Laboratories, Burlingame, CA, USA) and preparations observed and photographed using a Zeiss-Axioplan 2 fluorescence microscope (Carl Zeiss Italy, Arese, Italy).

Mesangial cell ROS levels ROS levels were assessed by evaluating formation of the intracellular trapped fluorescent compound resulting from the oxidation of 5-(and-6)-chloromethyl-2′,7′-dichlorodihydrofluorescein diacetate (CM-H_2DCFDA; Molecular Probes) by several ROS, including

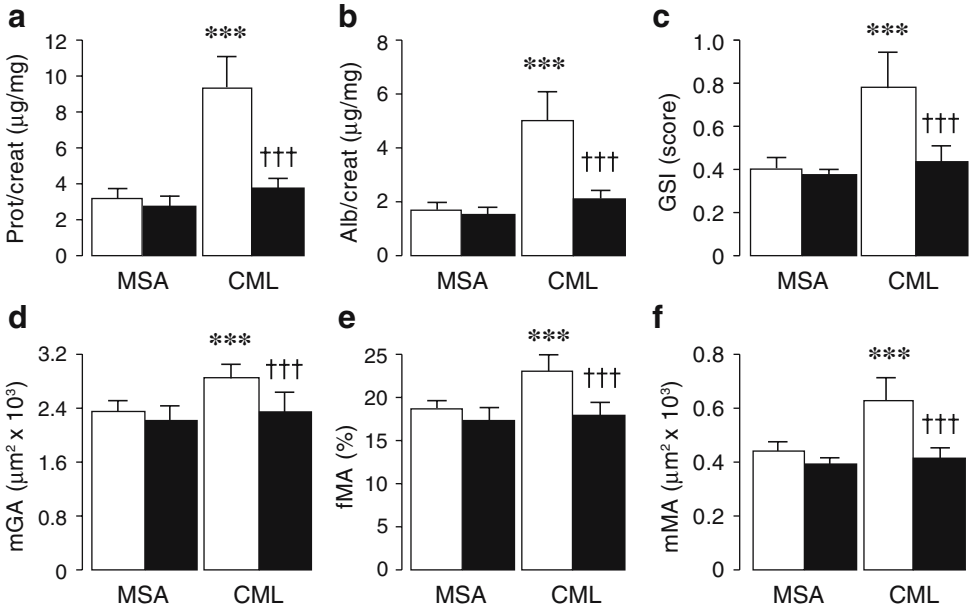

Fig. 1 Urinary protein:creatinine ratio (Prot/creat; **a**), urinary albumin:creatinine ratio (Alb/creat; **b**), GSI (**c**), mGA (**d**), fMA (**e**) and mMA (**f**) in WT (*white bars*) and $p66^{Shc}$ KO (*black bars*) mice injected with MSA or CML-modified MSA (means±SD; $n=7$ per group). ***$p<0.001$ in CML-treated vs the corresponding MSA-treated mice; †††$p<0.001$ in KO vs the corresponding WT mice

hydrogen peroxide [34]. Briefly, cells were incubated with 5 μmol/l CM-H_2DCFDA in serum-free medium for 30 min at 37°C, fixed in paraformaldehyde [2% (vol./vol.)] and observed under a fluorescence microscope (Zeiss-Axioplan 2) at 488 nm excitation and 530 nm emission.

Statistical analysis Results are expressed as mean±SD and percent change vs controls. Statistical significance was evaluated by one-way ANOVA followed by the Student–Newman–Keuls test for multiple comparisons. A p value of <0.05 was considered significant. All statistical tests were performed on raw data.

Results

In vivo studies Body weights did not differ between experimental animal groups, either at the beginning or at the end of the study period (data not shown).

While serum creatinine levels did not differ significantly between groups (not shown), glomerular barrier function was impaired in CML-treated WT mice only, with both the protein/creatinine and the albumin/creatinine ratios increasing approximately threefold vs the corresponding MSA-injected animals (Fig. 1a,b).

Kidney weights did not differ significantly among between groups, either at baseline or at the end of the study (not shown). Morphological evaluation of kidneys from WT-CML mice showed significant glomerular sclerosis, with PAS-positive deposits within the mesangium and thickening of glomerular basement membrane and Bowman's capsules. These changes were observed only rarely in kidney sections from KO-CML mice (Fig. 2). The glomerular sclerosis index increased significantly in WT-CML (approx. twofold increment), but not in KO-CML mice vs the corresponding MSA-treated animals (Fig. 1c).

At morphometric evaluation, mGA (Fig. 1c), mGV (not shown), fMA (Fig. 1e) and mMA (Fig. 1f) increased significantly in WT-CML vs WT-MSA mice (21, 34, 23 and 43% increase, respectively), but not in KO-CML vs KO-MSA animals.

Glomerular staining for active caspase-3 was very low in MSA-treated animals and increased significantly only in WT mice injected with CML (68% increase vs KO-CML), with predominant involvement of podocytes, though mesangial cells were not spared (Fig. 3a–c).

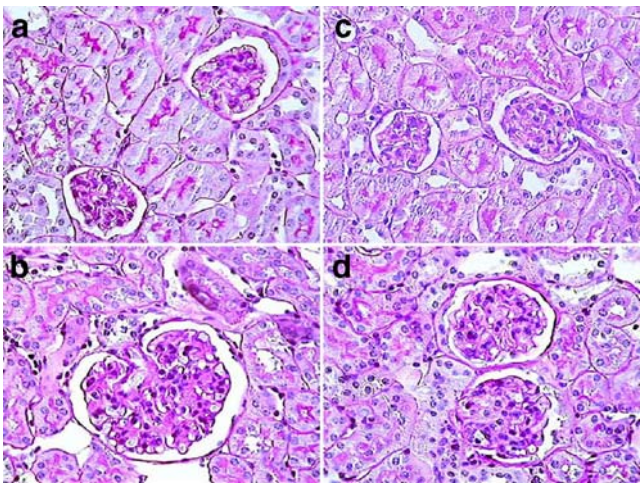

Fig. 2 Histological appearance of kidney sections from representative WT and $p66^{Shc}$ KO mice injected with MSA (**a**,**b**) or CML-modified MSA (**c**,**d**) (PAS; original magnification: ×400)

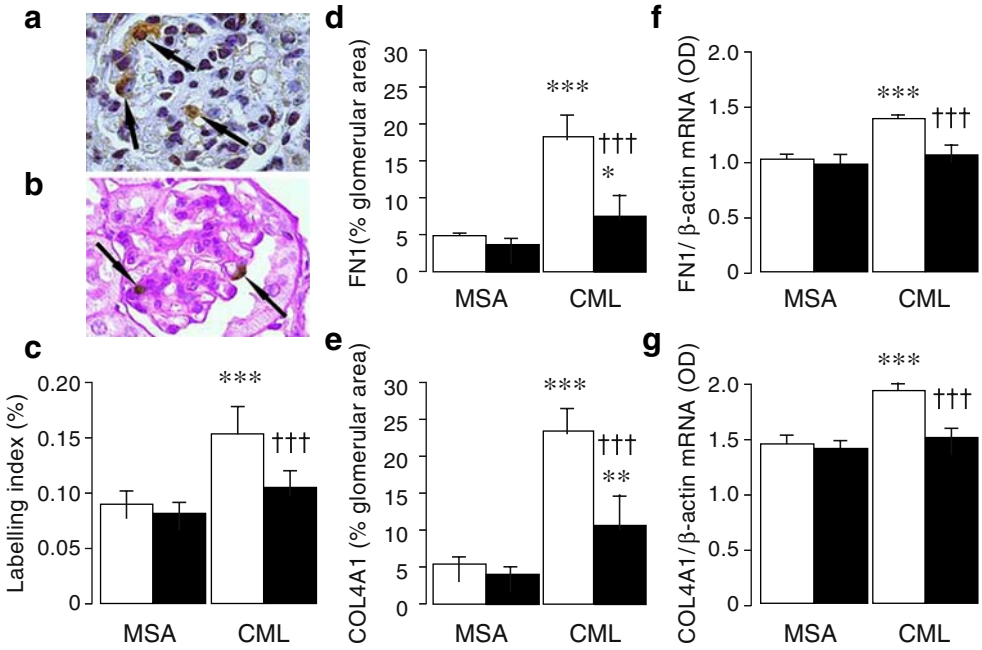

Fig. 3 Immunohistochemistry for active caspase-3 in two representative WT mice injected with CML-modified MSA without (**a**) and with (**b**) PAS counterstaining (original magnification: ×1,000) and quantification of glomerular cell death rate (**c**) and FN1 and COL4A1 protein (**d**,**e**) and corresponding mRNA (**f**,**g**) levels in WT (*white bars*) and *p66*^{Shc} KO (*black bars*) mice injected with MSA or CML-modified MSA (means± SD; n=4 per group). *p<0.05, **p<0.01 or ***p<0.001, in CML-treated vs the corresponding MSA-treated mice; †††p<0.001 in KO vs the corresponding WT mice

Glomerular staining for fibronectin and collagen IV increased significantly in both genotypes treated with CML, though increases were less pronounced (approx. twofold vs approx. fourfold increments) in KO than in WT mice [Fig. 3d,e; Supplementary Figs. 1 and 2]. Conversely, kidney cortex transcripts for *Fn1* and *Col4a1* increased slightly, but significantly, in WT-CML only (37 and 32% increase, respectively, vs WT-MSA; Fig. 3f,g).

Circulating and renal tissue AGE levels increased in mice from both genotypes treated with CML. Increments over the corresponding MSA-treated mice were significantly lower in KO than in WT mice (2.33-fold and 1.96-fold, respectively, vs 3.63-fold and 3.87-fold; Table 1); however, the renal clearance of AGEs did not differ significantly between the two CML-treated groups (not shown). Plasma isoprostane 8-epi-$PGF_{2\alpha}$ levels increased in WT-CML vs WT-MSA mice (+44%), whereas the increment detected in KO-CML vs KO-MSA mice (12%) did not achieve statistical significance (Table 1). Staining for CML and HNE was slightly positive only at the tubular level in MSA-treated mice. Tubular immunoreactivity increased markedly in animals from both genotypes injected with CML, though it was less intense and diffuse in KO than WT mice. At the glomerular level, positivity for these glycoxidation and lipoxidation products was observed only in WT mice treated with CML (Fig. 4).

RAGE and GAL3 immunostaining was negligible or absent in glomeruli from MSA-treated animals. In response to CML injection, RAGE protein levels were significantly increased in WT only (approx. fourfold increment), being localised mainly in podocytes (Fig. 5a, Supplementary Fig. 3), whereas GAL3 increased in both genotypes, though slightly less in KO vs WT mice (Fig. 5b, Supplementary Fig. 4). Kidney cortex *Rage* mRNA levels increased significantly only in WT-CML vs WT-MSA mice (53 and 39%, respectively, Fig. 5c), whereas *Gal3* mRNA expression was upregulated in both genotypes, though less in KO-CML than in WT-CML mice (Fig. 5d).

Table 1 Serum and kidney tissue AGEs, plasma isoprostane 8-epi-$PGF_{2\alpha}$ levels and renal NF κB/p65 activation in WT and *p66*^{Shc} KO mice injected with MSA or CML

	WT-MSA	KO-MSA	WT-CML	KO-CML
Serum AGEs (U/ml)	2.74±0.60	2.36±0.41	9.94±1.06[a]	5.50±0.55[a,b]
Kidney AGEs (U/mg)	7.78±0.99	6.14±0.49	30.11±2.53[a]	12.02±1.24[a,b]
Isoprostane 8-epi-$PGF_{2\alpha}$ (pg/ml)	83.63±7.06	77.29±5.09	120.11±8.74[a]	86.75±7.11[b]
NFκB/p65 activation (OD)	0.153±0.021	0.135±0.035	0.543±0.097[a]	0.188±0.036[b]

Values are means±SD; n=7 per group, except for NFκB/p65 activation (n=4)
[a] p<0.001 in CML-treated vs the corresponding MSA-treated mice
[b] p<0.001 in KO vs the corresponding WT mice

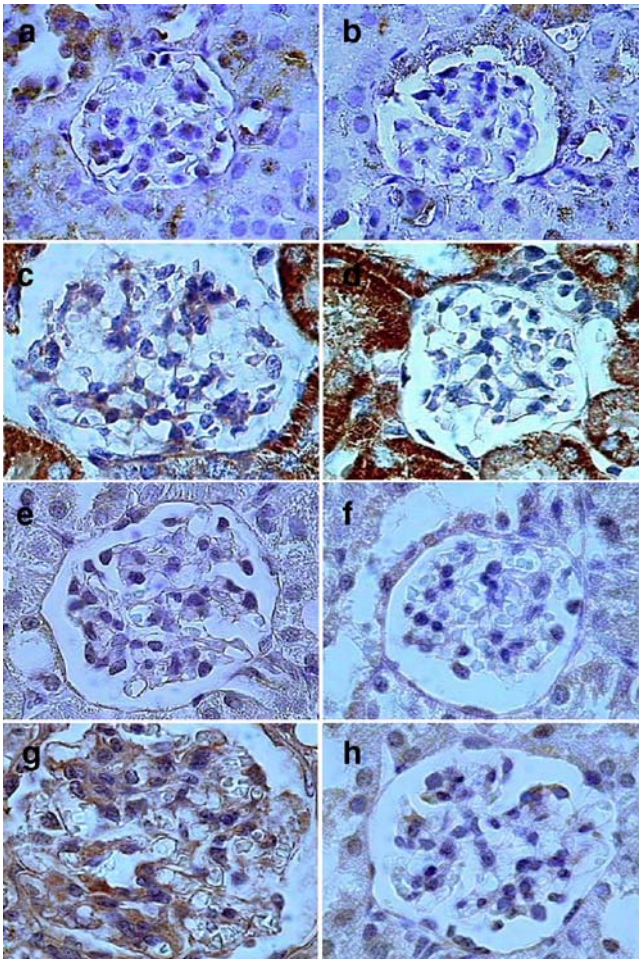

Fig. 4 Immunohistochemistry for CML (**a**–**d**) and 4-hydroxy-2-nonenal (**e**–**h**) in kidney sections from representative WT and *p66*^{Shc} KO mice injected with MSA or CML (original magnification: ×1,000). WT-MSA (**a**,**e**); KO-MSA (**b**,**f**); WT-CML (**c**,**g**); KO-CML (**d**,**h**)

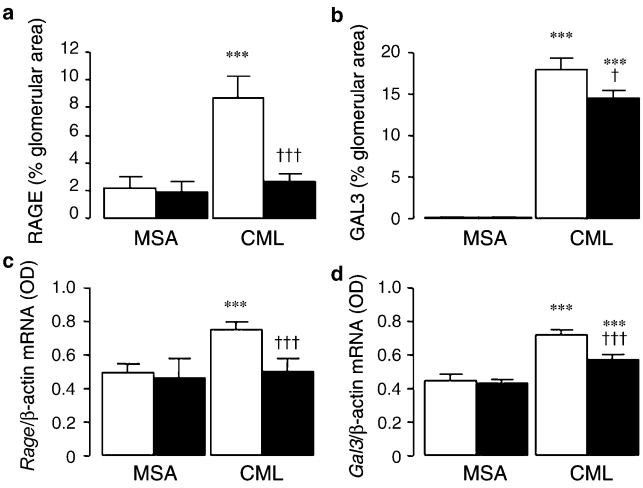

Fig. 5 Glomerular RAGE and GAL3 protein (**a**,**b**) and corresponding mRNA (OD ratio to β-actin mRNA (**c**,**d**) expression in WT (*white bars*) and *p66*^{Shc} KO (*black bars*) mice injected with MSA or CML-modified MSA (means±SD; n=4 per group).***p<0.001 in CML-treated vs the corresponding MSA-treated mice; †p<0.05 or †††p<0.001 in KO vs the corresponding WT mice

Both NOX4 (Fig. 6a–e) and *Nox4* mRNA (Fig. 6f) levels were significantly increased in CML-treated WT, but not KO mice vs the corresponding MSA-treated control animals. The activation of the redox-sensitive transcription factor NFκB/p65 within the kidney tissue increased in CML-treated vs MSA-treated WT (3.5-fold increment), but not in KO mice (Table 1).

The kidney cortex *p66*^{Shc} mRNA levels increased significantly (42%) in WT mice treated with CML vs those receiving MSA (data not shown).

No significant difference was detected in MSA-treated vs normal control animals for any of the measured parameters (not shown).

In vitro studies Since the in vivo assessment of the effect of *p66*^{Shc} deletion on CML-induced ROS generation and NF-κB activation was somewhat confounded by the lower AGE levels observed in KO vs WT mice, we conducted in vitro studies to verify that the reduced glyco- and lipo-oxidative markers and NF-κB activation were attributable to a blunted cellular response to CML in mice lacking *p66*^{Shc}.

ROS-dependent fluorescence was virtually undetectable in mesangial cells from both genotypes incubated with MSA. When exposed to CML, ROS levels increased markedly in cells from WT mice, but not in those from KO mice (Fig. 7a–d).

Likewise, significant nuclear translocation of NFκB/p65 was observed in WT cells exposed to CML, whereas it was only rarely observed in cells from KO mice (Fig. 7e–h). Prevention of NFκB activation in mesangial cells from KO mice was confirmed by the use of the ELISA-based method [0.192±0.018 vs 0.576±0.076 optical density (OD) in WT cells, p<0.001].

Discussion

The main finding of this study was that mice with a central regulator of oxidative stress, p66^{Shc}, knocked out are protected from renal disease induced by the glycoxidation product CML, as evidenced by the lack of significant proteinuria, glomerular hypertrophy, mesangial expansion and glomerular sclerosis, in contrast to the corresponding WT mice.

Glomerulopathy in CML-treated WT mice was accompanied by enhanced cell death rates and ECM protein production as well as by markedly increased serum and tissue AGE and plasma isoprostane 8-epi-PGF$_{2\alpha}$ levels, renal/glomerular CML and HNE content, and *Rage* and *Gal3* expression and levels of their respective proteins, as previously shown in mice rendered diabetic by injection of

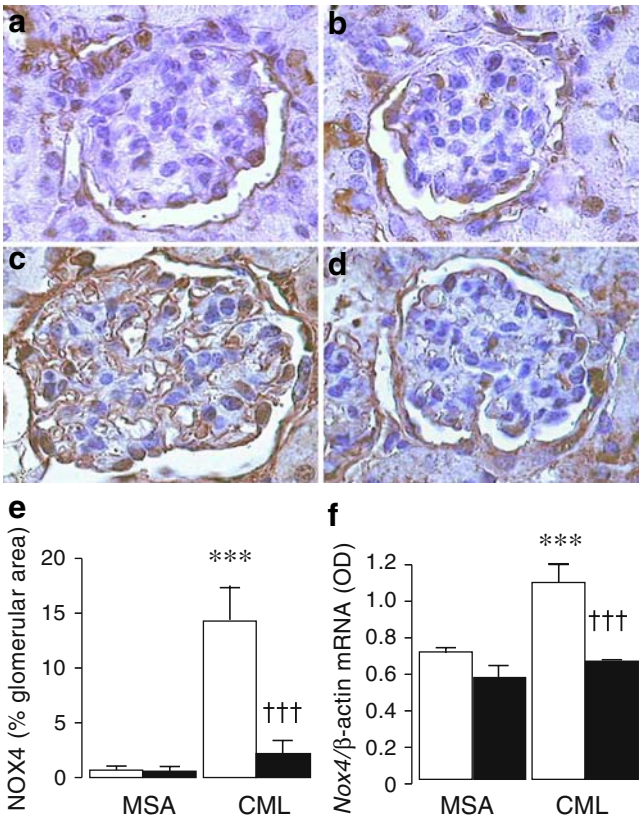

Fig. 6 Immunohistochemistry for Nox4 in kidney sections from representative WT and *p66*^{Shc} KO mice injected with MSA (**a**,**b**) or CML-modified MSA (**c**,**d**; original magnification: ×1,000). Quantification of glomerular NOX4 protein levels (**e**) and corresponding mRNA expression (OD ratio to β-actin mRNA level; **f**) in WT (*white bars*) and *p66*^{Shc} KO (*black bars*) mice injected with MSA or CML (means±SD; n=5 per group). ***p<0.001 in CML-treated vs the corresponding MSA-treated mice; †††p<0.001 in KO vs the corresponding WT mice

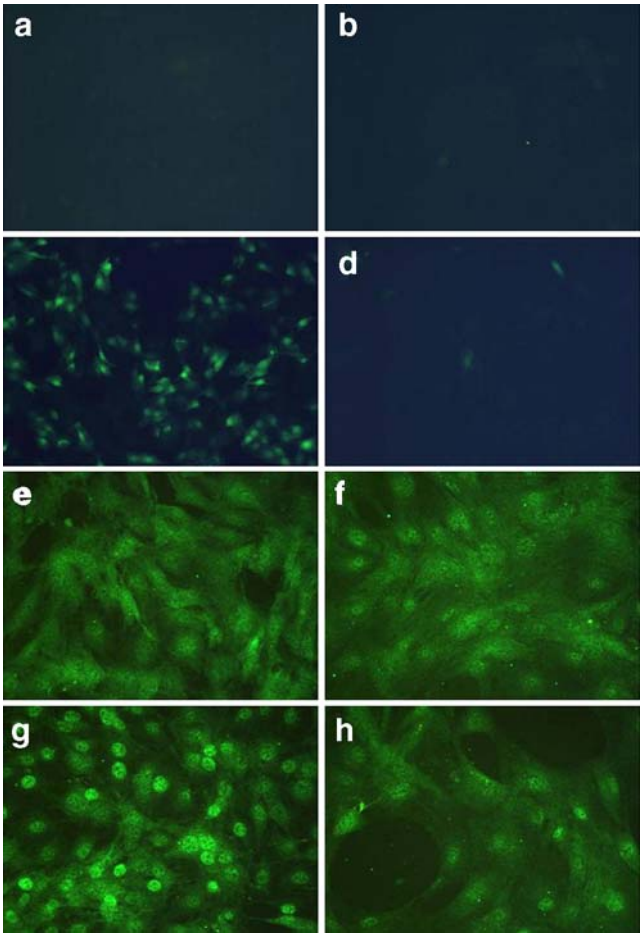

Fig. 7 Representative photographs of CM-H_2DCFDA (**a**–**d**) and NFkB/p65 (**e**–**h**) fluorescence in mesangial cells from WT and *p66*^{Shc} KO mice exposed for 1 h to serum-free media containing 100 μg/ml unmodified MSA or CML-modified MSA. WT-MSA (**a**,**e**); KO-MSA (**b**,**f**); WT-CML (**c**,**g**); KO-CML (**d**,**h**)

streptozotocin [34]. In addition, WT mice treated with CML displayed increased renal mRNA levels of *p66*^{Shc}, in keeping with previous reports showing the upregulation of p66^{Shc} production and expression of the gene in diabetic humans [42] and animals [34]. Conversely, CML-treated KO mice showed no increment in glomerular cell death rate and less marked matrix deposition within the glomerulus. Moreover, circulating and tissue levels of AGEs and glomerular GAL3 protein production were less pronounced than those detected in the WT mice, with no increase in plasma isoprostanes 8-epi-$PGF_{2\alpha}$, levels, renal/glomerular CML and HNE content and *Rage* mRNA expression and RAGE levels vs the corresponding MSA-treated animals.

These findings indicate that ablation of the *p66*^{Shc} gene prevented the development of CML-induced glomerulopathy by virtually abrogating the oxidative response to CML treatment. The attenuation of CML-induced oxidative stress might also be responsible for the lower circulating and tissue AGE levels observed in *p66*^{Shc} KO vs the corresponding WT mice, despite injection of equal amounts of CML, due to several mechanisms. These mechanisms include: (1) reduced AGE formation through ROS-dependent mechanisms, involving oxidative (or nonenzymatic, with ROS-dependent formation of carbonyl precursors and AGEs such as glyoxal, pentosidine and CML) and also nonoxidative (or enzymatic, due to ROS-dependent inhibition of GAPDH leading to diversion of glycolysis toward methylglyoxal formation) pathways; (2) increased AGE disposal via AGE receptor (namely RAGE)-dependent pathways; and (3) the possibility of enhanced catabolism by detoxifying enzymes such as aldose reductase and glyoxalase, due to the increased availability of their cofactors NADPH and reduced glutathione, respectively, as a consequence of reduced oxidative stress. Moreover, the observation that ROS generation (and consequent NFκB activation) induced by CML was almost completely prevented in mesangial cells from KO mice, as compared with those from WT animals, suggests that lack of p66^{Shc} protein directly inhibited CML action and the consequent activation of redox-dependent signalling pathways leading to changes in matrix and cell turnover, i.e. the

two major processes underlying mesangial expansion and glomerular sclerosis. Taken together, our data are consistent with the concept that extensive AGE formation occurring in ageing, diabetes and other age-related disorders through several pathways, including ROS-dependent mechanisms, plays a pivotal role in the pathogenesis of renal disease associated with these conditions via induction of (RAGE-mediated) oxidative stress and injury, thus suggesting the existence of a vicious circle linking ROS and AGEs. Conversely, ROS-independent effects do not appear to contribute significantly to AGE-induced renal tissue injury. This observation is in agreement with previous studies, indicating that interventions aimed at reducing oxidative stress are effective in preventing different types of experimental renal disease [43–46] and that amelioration of diabetic and nondiabetic renal and cardiovascular disease observed in the *p66^{Shc}* KO mouse model is associated with reduction of oxidative stress [34–38].

These data also demonstrate that p66^{Shc} is involved in the regulation of AGE-induced generation of intracellular ROS and activation of signalling pathways leading to oxidant-dependent renal tissue injury, as previously shown for other pro-oxidant stimuli [31, 32, 34, 37]. More importantly, these data provide novel information about the molecular mechanisms underlying p66^{Shc} action. In fact, the finding that *p66^{Shc}* ablation was associated with abrogation of CML-induced upregulation of production of the renal NAD(P)H isoform and expression of the *Nox4* gene indicates that p66^{Shc} modulates production of this ROS-generating enzyme. Recently, p66^{Shc} was also found to interact with the NAD(P)H oxidase activator Rac1 GTPase in a bidirectional fashion. Rac1 was reported to induce p38/MAPK-mediated phosphorylation of serine 54 and threonine 386 in p66^{Shc}, thus inhibiting its ubiquitination and increasing protein stability [47]. Conversely, the NH_2-terminal proline-rich collagen homology 2 domain of p66^{Shc} was shown to associate in vitro with full-length growth factor receptor bound protein (Grb2), thus competing with the proline-rich COOH-terminal region of son of sevenless 1 protein (Sos1). As a consequence Grb2 dissociates from Sos1, which is enabled to function as a guanine nucleotide exchange factor to activate Rac1 [48]. Therefore, p66^{Shc} is capable of enhancing both the production and activity of NAD(P)H oxidase, thus increasing ROS generation at the cytosolic level. However, since p66^{Shc} was shown to oxidise cytochrome *c* in response to stress signals, thus generating proapoptotic hydrogen peroxide within the mitochondrion [33], both ROS sources, cytosolic and mitochondrial, appear to be responsible for AGE-induced p66^{Shc}-dependent oxidative stress. This is in keeping with the prevention of high glucose-induced ROS upregulation in mesangial cells [34] and podocytes [49] and AGE-stimulated oxidative stress in endothelial cells [21] by inhibitors of either NAD(P)H oxidase or the mitochondrial respiratory chain.

Finally, the finding that CML-induced NFκB activation was abrogated by p66^{Shc} ablation in kidneys and mesangial cells indicates that this redox-sensitive transcription factor plays a major role as a downstream effector of ROS-dependent signalling pathways leading to oxidative injury. This conclusion is in keeping with the NFκB transcription programme, which includes several target genes that participate in the control of cell cycle, apoptosis, oxidative stress, immunity, inflammation and repair, all functions that are profoundly altered during renal disease of various causes [50]. NFκB activation may in turn amplify p66^{Shc}-dependent phenomena by regulating the expression of pro-oxidant genes.

In conclusion, these data show that p66^{Shc} ablation is associated with protection from the development of AGE-induced glomerulopathy. This protection appears to be dependent on a reduced susceptibility to AGE accumulation and AGE-induced tissue injury through ROS-dependent mechanisms involving NFκB activation, with consequent negative regulation of apoptosis and ECM deposition. Modulation of NAD(P)H oxidase production represents an additional mechanism by which p66^{Shc} regulates intracellular ROS levels. In addition, these results suggest that an intervention targeted to p66^{Shc} might be effective in the prevention and treatment of renal disease associated with age-related, AGE-dependent disorders.

Acknowledgements This work was supported by grants from the European Foundation for the Study of Diabetes/Servier, the Ministry of University and Research of Italy (40%) and the Diabetes, Endocrinology and Metabolism Foundation, Rome, Italy.

Duality of interest The authors declare that there is no duality of interest associated with this manuscript.

References

1. Vlassara H, Striker LJ, Teichberg S, Fuh H, Li YM, Steffes MW (1994) Advanced glycation endproducts induce glomerular sclerosis and albuminuria in normal rats. Proc Natl Acad Sci USA 91:11704–11708
2. Vlassara H, Fuh H, Makita Z, Krungkrai S, Cerami A, Bucala R (1992) Exogenous advanced glycosylation end products induce complex vascular dysfunction in normal animals: a model for diabetic and aging complications. Proc Natl Acad Sci USA 89:12043–12047
3. Vlassara H, Fuh H, Donnelly T, Cybulsky M (1995) Advanced glycation endproducts promote adhesion molecule (VCAMf-1, ICAM-1) expression and atheroma formation in normal rabbits. Mol Med 1:447–456
4. Soulis-Liparota T, Cooper M, Papazoglou D, Clarke B, Jerums G (1991) Retardation by aminoguanidine of development of albu-

minuria, mesangial expansion, and tissue fluorescence in streptozotocin-induced diabetic rat. Diabetes 40:1328–1334
5. Forbes JM, Yee LT, Thallas V et al (2004) Advanced glycation end product interventions reduce diabetes-accelerated atherosclerosis. Diabetes 53:1813–1823
6. Candido R, Forbes JM, Thomas MC et al (2003) A breaker of advanced glycation end products attenuates diabetes-induced myocardial structural changes. Circ Res 92:785–792
7. Li YM, Steffes M, Donnelly T et al (1996) Prevention of cardiovascular and renal pathology of aging by the advanced glycation inhibitor aminoguanidine. Proc Natl Acad Sci USA 93:3902–3907
8. Schleicher ED, Wagner E, Nerlich AG (1997) Increased accumulation of the glycoxidation product *N*(epsilon)-(carboxymethyl)lysine in human tissues in diabetes and aging. J Clin Invest 99:457–468
9. Sell DR, Nagaraj RH, Grandhee SK et al (1991) Pentosidine: a molecular marker for the cumulative damage to proteins in diabetes, aging, and uremia. Diabetes Metab Rev 7:239–251
10. Li SY, Liu Y, Sigmon VK, McCort A, Ren J (2005) High-fat diet enhances visceral advanced glycation end products, nuclear *O*-Glc-Nac modification, p38 mitogen-activated protein kinase activation and apoptosis. Diabetes Obes Metab 7:448–454
11. Metz TO, Alderson NL, Chachich ME, Thorpe SR, Baynes JW (2003) Pyridoxamine traps intermediates in lipid peroxidation reactions in vivo: evidence on the role of lipids in chemical modification of protein and development of diabetic complications. J Biol Chem 278:42012–42019
12. Wu L, Juurlink BH (2002) Increased methylglyoxal and oxidative stress in hypertensive rat vascular smooth muscle cells. Hypertension 39:809–814
13. Chen J, Muntner P, Hamm LL et al (2004) The metabolic syndrome and chronic kidney disease in U.S. adults. Ann Intern Med 140:167–174
14. McNeill AM, Rosamond WD, Girman CJ et al (2005) The metabolic syndrome and 11-year risk of incident cardiovascular disease in the atherosclerosis risk in communities study. Diabetes Care 28:385–390
15. Baynes JW, Thorpe SR (1999) Role of oxidative stress in diabetic complications: a new perspective on an old paradigm. Diabetes 48:1–9
16. Brownlee M (2005) The pathobiology of diabetic complications: a unifying mechanism. Diabetes 54:1615–1625
17. Van Remmen H, Richardson A (2001) Oxidative damage to mitochondria and aging. Exp Gerontol 36:957–968
18. Inoguchi T, Sonta T, Tsubouchi T et al (2003) Protein kinase C-dependent increase in reactive oxygen species (ROS) production in vascular tissues of diabetes: role of vascular NAD(P)H oxidase. J Am Soc Nephrol 14:S227–S232
19. Baynes JW, Thorpe SR (2000) Glycoxidation and lipoxidation in atherogenesis. Free Radic Biol Med 28:1708–1716
20. Huebschmann AG, Regensteiner JG, Vlassara H, Reusch JE (2006) Diabetes and advanced glycoxidation end products. Diabetes Care 29:1420–1432
21. Basta G, Lazzerini G, Del Turco S, Ratto GM, Schmidt AM, De Caterina R (2005) At least 2 distinct pathways generating reactive oxygen species mediate vascular cell adhesion molecule-1 induction by advanced glycation end products. Arterioscler Thromb Vasc Biol 25:1401–1407
22. Lander HM, Tauras JM, Ogiste JS, Hori O, Moss RA, Schmidt AM (1997) Activation of the receptor for advanced glycation end products triggers a p21(ras)-dependent mitogen-activated protein kinase pathway regulated by oxidant stress. J Biol Chem 272:17810–17814
23. Bierhaus A, Chevion S, Chevion M et al (1997) Advanced glycation end product-induced activation of NF-kappaB is suppressed by alpha-lipoic acid in cultured endothelial cells. Diabetes 46:1481–1490
24. Bierhaus A, Humpert PM, Stern DM, Arnold B, Nawroth PP (2005) Advanced glycation end product receptor-mediated cellular dysfunction. Ann N Y Acad Sci 1043:676–680
25. Ramasamy R, Vannucci SJ, Yan SS, Herold K, Yan SF, Schmidt AM (2005) Advanced glycation end products and RAGE: a common thread in aging, diabetes, neurodegeneration, and inflammation. Glycobiology 15:16R–28R
26. Yamagishi S, Inagaki Y, Okamoto T et al (2002) Advanced glycation end product-induced apoptosis and overexpression of vascular endothelial growth factor and monocyte chemoattractant protein-1 in human-cultured mesangial cells. J Biol Chem 277:20309–20315
27. Li L, Renier G (2006) Activation of nicotinamide adenine dinucleotide phosphate (reduced form) oxidase by advanced glycation end products links oxidative stress to altered retinal vascular endothelial growth factor expression. Metabolism 55:1516–1523
28. Yan SD, Schmidt AM, Anderson GM et al (1994) Enhanced cellular oxidant stress by the interaction of advanced glycation end products with their receptors/binding proteins. J Biol Chem 269:9889–9897
29. Wautier JL, Wautier MP, Schmidt AM et al (1994) Advanced glycation end products (AGEs) on the surface of diabetic erythrocytes bind to the vessel wall via a specific receptor inducing oxidant stress in the vasculature: a link between surface-associated AGEs and diabetic complications. Proc Natl Acad Sci USA 91:7742–7746
30. Migliaccio E, Mele S, Salcini AE et al (1997) Opposite effects of the $p52^{shc}$/$p46^{shc}$ and $p66^{shc}$ splicing isoforms on the EGF receptor-MAP kinase-fos signalling pathway. EMBO J 16:706–716
31. Migliaccio E, Giorgio M, Mele S et al (2000) The $p66^{shc}$ adaptor protein controls oxidative stress response and life span in mammals. Nature 402:309–313
32. Trinei M, Giorgio M, Cicalese A et al (2002) A p53-$p66^{Shc}$ signalling pathway controls intracellular redox status, levels of oxidation-damaged DNA and oxidative stress-induced apoptosis. Oncogene 21:3872–3878
33. Giorgio M, Migliaccio E, Orsini F et al (2005) Electron transfer between cytochrome *c* and $p66^{Shc}$ generates reactive oxygen species that trigger mitochondrial apoptosis. Cell 122:221–233
34. Menini S, Amadio L, Oddi G et al (2006) Deletion of $p66^{Shc}$ longevity gene protects against experimental diabetic glomerulopathy by preventing diabetes-induced oxidative stress. Diabetes 55:1642–1650
35. Rota M, LeCapitaine N, Hosoda T et al (2006) Diabetes promotes cardiac stem cell aging and heart failure, which are prevented by deletion of the p66shc gene. Circ Res 99:42–52
36. Francia P, Delli Gatti C, Bachschmid M et al (2004) Deletion of p66shc gene protects against age-related endothelial dysfunction. Circulation 110:2889–2895
37. Zaccagnini G, Martelli F, Fasanaro P et al (2004) $p66^{ShcA}$ modulates tissue response to hindlimb ischemia. Circulation 109:2917–2923
38. Napoli C, Martin-Padura I, de Nigris F et al (2003) Deletion of the $p66^{Shc}$ longevity gene reduces systemic and tissue oxidative stress, vascular cell apoptosis, and early atherogenesis in mice fed a high-fat diet. Proc Natl Acad Sci USA 100:2112–2116
39. Iacobini C, Menini S, Oddi G et al (2004) Galectin-3/AGE-receptor 3 knockout mice show accelerated AGE-induced glomerular injury. Evidence for a protective role of galectin-3 as an AGE-receptor. FASEB J 18:1773–1775
40. Gorin Y, Block K, Hernandez J et al (2005) Nox4 NAD(P)H oxidase mediates hypertrophy and fibronectin expression in the diabetic kidney. J Biol Chem 280:39616–39626
41. Cecchinelli B, Lavra L, Rinaldo C et al (2006) Repression of the antiapoptotic molecule galectin-3 by homeodomain-interacting protein kinase 2-activated p53 is required for p53-induced apoptosis. Mol Cell Biol 26:4746–4757

42. Pagnin E, Fadini G, de Toni R, Tiengo A, Calo L, Avogaro A (2005) Diabetes induces p66shc gene expression in human peripheral blood mononuclear cells: relationship with oxidative stress. J Clin Endocrinol Metab 90:1130–1136
43. Craven PA, Melhem MF, Phillips SL, DeRubertis FR (2001) Overexpression of Cu^{2+}/Zn^{2+} superoxide dismutase protects against early diabetic glomerular injury in transgenic mice. Diabetes 50:2114–2125
44. Kaneko K, Yonemitsu Y, Fujii T et al (2006) A free radical scavenger but not FGF-2-mediated angiogenic therapy rescues myonephropathic metabolic syndrome in severe hindlimb ischemia. Am J Physiol 290:H1484–H1492
45. Manning RD Jr, Tian N, Meng S (2005) Oxidative stress and antioxidant treatment in hypertension and the associated renal damage. Am J Nephrol 25:311–317
46. Budisavljevic MN, Hodge L, Barber K et al (2003) Oxidative stress in the pathogenesis of experimental mesangial proliferative glomerulonephritis. Am J Physiol 285:F1138–F1148
47. Khanday FA, Yamamori T, Mattagajasingh I et al (2006) Rac1 leads to phosphorylation-dependent increase in stability of the p66shc adaptor protein: role in Rac1-induced oxidative stress. Mol Biol Cell 17:122–129
48. Khanday FA, Santhanam L, Kasuno K et al (2006) Sos-mediated activation of rac1 by p66shc. J Cell Biol 172:817–822
49. Susztak K, Raff AC, Schiffer M, Böttinger EP (2006) Glucose-induced reactive oxygen species cause apoptosis of podocytes and podocyte depletion at the onset of diabetic nephropathy. Diabetes 55:225–233
50. Guijarro C, Egido J (2001) Transcription factor κB (NFκB) and renal disease. Kidney Int 59:415–424